

# UNIVERSITY OF TWENTE.

## **Assessing the Potential of Amyloid-Like Protein Fibrils in a Nanoplastic Filtration Model System**

The Pursuit of Sustainable Nanoplastic Filtration Strategies

**Emre Sinecek (S2696215)**

**Biomedical Engineering Bachelor Thesis**  
Nanobiophysics Group (NBP)

### **Committee Members:**

Dr. Christian Blum (Chair)

Dr. Slav Semerdzhiev (Supervisor)

Dr.ir. Kirsten Pondman (External member)

**Date submitted: 12/03/2025**

## Abstract

This thesis explores the use of amyloid-like protein fibrils as filtration materials for capturing nanoplastics. Fibril-modified membranes were prepared using five different proteins, with seven fibril aggregation methods tested to optimize their performance. Due to inconsistencies or poor performance, only  $\alpha$ -synuclein and lysozyme fibrils were selected for final experiments to evaluate their retention efficiency for varying concentrations of fluorescent nanobeads.

The results show that  $\alpha$ -synuclein achieved significantly higher retention efficiency, reaching up to 94%, compared to lysozyme, which reached only 22%. The observed retention trends deviated from those reported in the existing literature. However, these discrepancies may be justified by considering the differences in fibril network density, structural integrity, and interaction strength, all of which may influence retention efficiency.

During experimentation, issues related to membrane integrity and fibril deposition arose. Imaging showed a buildup of fibrils at membrane edges and tearing under high pressure, which would later be remedied with a support layer. Furthermore, the number of data points should be increased to more accurately determine trends, and the limitation of the deposition method should be addressed to improve reliability.

## Acknowledgements

At the forefront of my gratitude is my lead supervisor, Dr. Slav Semerdzhiev, for his support, patience, and guidance throughout this thesis journey. His insights have helped shape the research presented here, and I am deeply grateful for his unwavering support.

I would also like to extend my sincere gratitude to Robert Molenaar. His assistance in determining the bead concentration was crucial to this research. His expertise and assistance with various technical issues on different occasions have also been invaluable.

My deepest appreciation goes to Dr. Christian Blum and Prof. Dr. Mireille Claessens for their advice and help during our weekly meetings, which was instrumental in steering this thesis toward its completion.

Special thanks to my friend Alistair Cooper, whose friendship and constant willingness to assist in any way possible have been of immense value.

Thank you all,

*Emre Sinecek*

# Contents

Abstract .....	2
Acknowledgements .....	3
1 Introduction .....	6
1.1 Nanoplastics: A Growing Environmental Challenge.....	6
1.2 Currently used techniques for MP removal .....	6
1.2.1 Coagulation and Flocculation.....	6
1.2.2 Rapid Sand Filtration .....	7
1.2.3 Ultrafiltration Membranes .....	7
1.3 Protein Fibrils as Functional Filtration Materials.....	8
1.4 Interaction Mechanisms Between Plastics and Protein Fibrils .....	8
1.5 Introduction Summary.....	9
1.5.1 Aims and Objectives .....	9
1.5.2 Hypothesis .....	9
2 Methodology .....	10
2.1 Experimental preparation .....	10
2.1.1 Fibril preparation conditions.....	10
2.1.2 Fibril incubation conditions .....	10
2.1.3 Detection of fibril formation and early selection process .....	11
2.1.4 Quantification of fibril concentration .....	11
2.1.5 Physical equipment .....	13
2.2 Experimental Data Collection .....	14
2.2.1 Spectrometer .....	14
3 Results and Discussion.....	15
3.1 Influence of membrane on fluorescent bead retention.....	15
3.1.1 Membrane-only retention of 500 nm beads.....	15
3.1.2 Membrane-only retention of 40 nm beads.....	17
3.2 Monitoring protein fibrillation using Thioflavin T assay.....	19
3.2.1 Characterizing Fibril Morphology with AFM.....	20
3.2.2 Preliminary Analysis of Protein Filter Performance.....	21
3.3 Evaluating Fibril Performance in Filtration.....	24
3.3.1 Retention Efficiency with Increasing Fibril Concentration .....	24
3.3.2 Quantifying fibril deposition .....	26
3.3.3 Visualizing Fibril Deposition and Membrane Stability .....	27

3.4 Determining protein retention performance trends .....	29
3.4.1 $\alpha$ -Synuclein fibril-modified membrane.....	30
3.4.2 Lysozyme fibril-modified membrane .....	30
4 Conclusion.....	33
References.....	34

# 1 Introduction

This thesis is organised into four main chapters, each containing subchapters. Chapter 1 is an introduction into the growing concerns associated with nanoplastics. It also examines existing literature, regarding the effect of nanoplastics on their environment, ways in which they are currently being processed, and shows research objectives and hypotheses. Chapter 2 showcases the methodology used in the thesis, specifically the experimental design and procedure. Chapter 3 presents the various findings of the study and analyses these findings critically. This chapter also goes over the experimental limitations. Chapter 4 concludes the study, summarizing key findings and the direction for future research.

## 1.1 Nanoplastics: A Growing Environmental Challenge

Plastics are synthetic materials derived from fossil fuels. They are versatile, durable, and low-cost. In the present day, plastics can be found everywhere. Single-use plastics, such as packaging, bottles, and bags, are among the largest contributors to plastic waste, accounting for nearly 40% of global plastic production (Geyer et al., 2017). Additionally, microplastics from synthetic textiles, personal care products, and industrial abrasives are increasingly recognized as major pollutants, entering ecosystems and accumulating in food chains [1].

One of the primary reasons that plastics pose a great environmental threat is that they are non-biodegradable, meaning they do not decompose like natural materials and can persist in environments. Globally, over 8.3 billion tons of plastic have been created since their inception in the 1950s [2], around 9% of which has been recycled, 12% incinerated, while the other 79% remains in the environment [2].

When plastics degrade, they fracture into smaller particles called microplastics (MPs). These are plastics smaller than 5 mm in length [3]. These MPs are already small enough to be found in placentas [4], raising concerns about long-term health impacts.

Nanoplastics (NPs), plastic particles smaller than 1  $\mu\text{m}$ , have become and will remain a problem for the environment in the foreseeable future. Due to their size, they can travel through air and water undetected into different ecosystems, penetrate biological barriers (i.e., blood-brain barrier) [5], play a role in oxidative stress and toxicity [6], and become difficult to detect, monitor, or remove using traditional filtration techniques [7].

Earlier attempts to address pollution of NPs have mainly relied on mechanical and chemical filtration methods, but these methods often proved difficult to be efficient, scalable or environmentally sustainable enough.

## 1.2 Currently used techniques for MP removal

### 1.2.1 Coagulation and Flocculation

Another common method of MP removal from water are coagulation processes combined with flocculation. This involves adding chemicals to the water which make MPs clump together which can then be removed more easily using traditional filtration methods. Flocculation involves a stirring movement to promote this clumping. The process does leave a sludge containing MPs [8].

A study by Jachimowicz and Cydzik-Kwiatkowska (2022) showed the effects of different coagulants on the removal of MP in wastewater, reaching up to 90% efficiency when using PAX [8]. Specific coagulants and flocculants can improve the removal of certain pollutants; however, this sometimes requires high doses [8], therefore increasing the chances at secondary pollution.

At its nature this method involves putting chemicals in water, which may create secondary pollution, and depending on the coagulants used has variable efficiency. Coagulation currently only works as a method of MP removal and can be very efficient. Their efficiency with regards to the removal of smaller NPs remains untested and unknown, due to the NPs inherent ability to remain undetected. Moreover, the sludge that is created still needs go through further stages of sludge post-treatment disposal, which is an inherently environmentally unsustainable process.

### 1.2.2 Rapid Sand Filtration

Rapid sand filtration (RSF) is the most-used filtration techniques for the removal of MPs due to its low operational and maintenance costs [9]. Rapid sand filters use granular media like sand and anthracite in layered beds to remove larger particles. MPs adhere to the granular media surfaces through hydrophilic interactions.

RSF removed about 97% of MPs of all shapes, sizes, has more efficient reduction when used in conjunction with pre-emptive coagulation and flocculation. When just the RSF process was utilized by itself, the removal efficiency was only 73.8%. When used in conjunction with the coagulation process it reached up to 98.9% [10], but this introduces the negatives tied to coagulation and flocculation as previously described. The MPs tested in this case were only 20-100  $\mu\text{m}$  in size [11], well clear of the starting sizes of NPs ( $< 1 \mu\text{m}$ ). Once again, the effect of this technique on the removal of NPs is unknown.

### 1.2.3 Ultrafiltration Membranes

Ultrafiltration (UF) membranes are a promising technology for the removal of MPs and NPs from water due to their ability to filter particles in the size range of 0.01–0.1  $\mu\text{m}$ . UF membranes operate under pressure-driven processes, where water is forced through a semi-permeable membrane, effectively retaining particles larger than the membrane's pore size. This method is especially advantageous for NPs, as their small size makes them difficult to remove using conventional techniques like coagulation or rapid sand filtration [24].

A study by Enfrin et al. (2020) demonstrated that UF membranes could achieve over 99% removal efficiency for MPs and NPs, even at high concentrations [25]. However, the study also highlighted challenges such as membrane fouling, where MPs and NPs accumulate on the membrane surface, reducing filtration efficiency over time. Fouling can lead to increased operational costs due to the need for frequent membrane cleaning or replacement [25]. To mitigate this, hybrid systems combining UF with pre-treatment methods like coagulation have been explored. For example, Zhang et al. (2021) reported that pre-coagulation improved UF membrane performance, reducing fouling and enhancing NP removal efficiency [26].

Despite its high efficiency, UF has limitations. The energy consumption associated with maintaining the required pressure for filtration can be significant, making it less sustainable for large-scale applications [27]. Additionally, the disposal of used membranes, which are often made of non-biodegradable polymers, poses an environmental challenge. Research is ongoing

to develop more sustainable and fouling-resistant membranes, such as those incorporating nanomaterials or biodegradable polymers [28].

### 1.3 Protein Fibrils as Functional Filtration Materials

Amyloid-like protein fibrils have gained attention in the field of environmental rehabilitation due to their structural and chemical properties. They are self-propagating nanostructures with exceptional stability and mechanical strength as a result of their characteristic structure [12]. Protein fibrils are biodegradable, biocompatible, and made from renewable sources, making them a sustainable alternative to filter materials [13].

Amyloid fibrils have a high surface area and contain intrinsically hydrophobic and hydrophilic domains, which allows them to bind to a wide range of contaminants, including plastics. In addition to these domains, amyloid fibrils also display charged functional groups on their surface. This enables electrostatic interactions with contaminants that are oppositely charged, which includes nanoplastics. These interactions can enhance the fibrils' ability to capture pollutants, as shown in the works of Gabbrielli et al. (2023) [14]. Other studies have shown further versatility of these fibrils when capturing various micropollutants, both biological pollutants like bacteria and chemical ones like per- and polyfluoroalkyl substances (PFAS) [15, 16]. Moreover, amyloid fibrils can be chemically functionalized to increase their specificity and adsorption capacity for particular contaminants, which makes them adaptable for targeted applications.

Therefore, fibrils can act as sticky, high surface area material to trap NPs by binding to their surface through multivalent interactions. Amyloid fibrils also show potential for scaling into functional filtration systems by integrating them into membranes, which improves their practical usability. Their nanoscale architecture enables selective adsorption, and their ability to self-assemble into stable networks makes them suitable for diverse environmental conditions.

### 1.4 Interaction Mechanisms Between Plastics and Protein Fibrils

To optimize the performance of protein-based filtration methods, an understanding of the interactions between protein fibrils and NPs is crucial. Molecular dynamics simulations, like those conducted by Gabbrielli et al. (2023) [14], show that nanoplastic adsorption onto fibrils is mediated by a combination of hydrophobic interactions, van der Waals forces, and electrostatic attractions. These interactions are influenced both by the physicochemical properties of the NPs like shape, size, and surface charge, and the surface chemistry of the fibrils. For example, regions of protein fibrils have been shown to interact strongly with non-polar plastic surfaces, while charged functional groups enhance binding to polar or charged plastic particles [9]. By tuning these surface properties, it may be possible to design fibrils that show high selectivity and binding efficiency for specific nanoplastic pollutants.

Recent studies have explored the use of protein fibrils for MP and NP removal, highlighting their potential as sustainable filtration materials. Peydayesh et al. (2021) made use of protein amyloid fibrils in combination with coagulation-flocculation to facilitate the removal of microplastics and natural organic matter from water in a sustainable manner [29]. The study introduced lysozyme amyloid fibrils as sustainable bio-flocculant for water purification, achieving up to 98.2% removal efficiency for polystyrene MPs. Electrostatic interactions and the fibrils' high surface area were highlighted as they played a critical role in capturing MPs, even under natural water conditions. As

amyloid fibrils are biodegradable, they do not introduce secondary pollution like with traditional flocculation methods.

## 1.5 Introduction Summary

NPs, plastic particles smaller than 1  $\mu\text{m}$ , present an ever-growing environmental challenge due to their persistence, ability to penetrate biological barriers, and ability to avoid detection and removal [3, 5, 7]. Existing filtration techniques, such as UF membranes, offer high removal efficiencies but face challenges like membrane fouling and environmental concerns regarding disposal [27]. Alternative methods, including coagulation-flocculation and RSF are effective for removal of larger MPs but lack the proven efficiency for NPs and may introduce secondary pollution [8, 10].

Amyloid-like protein fibrils may provide a sustainable, biodegradable alternative due to their high surface area, structural ability, and ability to bind pollutants through multivalent interactions [12, 15, 16]. These fibrils can be chemically functionalized to enhance binding specificity to be used in targeted applications [15, 16]. However, as detection of NPs is made very difficult by their characteristics, studies on the effects of filtration on them are very limited. Experimental studies have shown that protein fibrils, such as lysozyme amyloid fibrils, can effectively remove MPs when used in bio-flocculation. They can achieve high removal efficiencies while avoiding the drawbacks of traditional chemical treatments [29].

### 1.5.1 Aims and Objectives

This study will explore the use of protein fibrils for nanoplastic filtration.

### 1.5.2 Hypothesis

The author of this study hypothesizes the following:

- I. Nanoplastic retention will increase with increasing amounts of protein fibrils deposited.
- II. Membrane pore size will influence nanoplastic retention due to size exclusion effects.

## 2 Methodology

This chapter will describe the methodology used in the creation of protein fibrils, the deposition of these fibrils onto membranes to create a protein filter, and the steps taken to acquire and compare each of these filters in terms of particle filtration efficiency.

### 2.1 Experimental preparation

#### 2.1.1 Fibril preparation conditions

Aggregation of the fibrils was initiated with preparations specific to each protein as shown in Table 1. Lysozyme and  $\beta$ -lactoglobulin both show up twice, as they have been prepared with both tris (pH 7.5) and glycine (pH 2).

Table 1: The reagents and their concentrations used to prepare specific proteins at specific conditions.

Proteins	Reagents				
	$C_{\text{protein}}$	Tris (pH 7.5)	Glycine (pH 2)	$\text{NaN}_3$	NaCl
$\alpha$ -Synuclein	250 $\mu\text{M}$	10 mM	-	0.02 wt%	10 mM
$\beta$ -lactoglobulin (pH 2)	550 $\mu\text{M}$	-	50 mM	0.02 mM	-
$\beta$ -lactoglobulin (pH 7.5)	550 $\mu\text{M}$	50 mM	-	-	-
Lysozyme (pH 2)	1 mM	-	100 mM	0.02 wt%	-
Lysozyme (pH 7.5)	1 mM	100 mM	-	0.02 wt%	-
BSA	6.6 mg/mL (~100 $\mu\text{M}$ )	20 mM	-	0.02 wt%	-
Insulin	2.2 mg/mL (~360 $\mu\text{M}$ )	-	50 mM	0.02 wt%	-

#### 2.1.2 Fibril incubation conditions

After preparation of aggregation, the proteins were incubated with conditions specific to each protein. This is shown in Table 2.

Table 2: Post-preparation incubation conditions specific to each protein type.

Proteins	Incubation conditions		
	Temperature	Shaking conditions	Time
$\alpha$ -Synuclein	37°C	400 rpm	4-5 days
$\beta$ -lactoglobulin (pH 2)	80°C	No shaking	24 hours
$\beta$ -lactoglobulin (pH 7.5)	80°C	No shaking	2-3 days
Lysozyme (pH 2)	65°C	No shaking	3-4 days

Lysozyme (pH 7.5)	65°C	No shaking	3-4 days
BSA	70°C	No shaking	4 days
Insulin	37 °C	700 rpm	3-4 days

### 2.1.3 Detection of fibril formation and early selection process

A Thioflavin T (ThT) assay is conducted to detect the capability of proteins to create fibrils. ThT dye is added to the sample containing amyloid fibrils at a 1:20 ratio, and a buffer solution (Tris). When ThT binds to these fibrils, it fluoresces. Since Tris should not be able to create fibrils, it should not fluoresce, it forms the negative control for this experiment. For this experiment, a 1:20 ratio of protein to ThT is used. The exact concentrations are shown in Table 3.

The ability of  $\alpha$ -synuclein to form fibrils is well documented and assessing it would be done through other means than ThT assay.

*Table 3: Protein and buffer (Tris) concentrations, and ThT concentrations maintained for ThT assay. Note that the ThT concentration for  $\beta$ -lactoglobulin preparations is rounded up from 27.5  $\mu$ M.*

	<b>Starting concentration</b>	<b>ThT concentration</b>
$\beta$ -lactoglobulin	550 $\mu$ M	30 $\mu$ M
Lysozyme	1 mM	50 $\mu$ M
BSA	100 $\mu$ M	5 $\mu$ M
Insulin	360 $\mu$ M	18 $\mu$ M
Tris	10 mM	500 $\mu$ M

### 2.1.4 Quantification of fibril concentration

To quantify how many of the proteins have formed fibrils, their respective fibril equivalent monomer concentration must be calculated. This was done by finding the absorbance of a spun down sample of the specific protein. Spinning at high g-forces causes the heavier fibrils to sink to the bottom, leaving only monomers at the supernatant area. A small sample of the aggregated solution would be taken and spun down in a centrifuge at 18,000 g for 30 minutes. The supernatant would be measured using a NanoDrop 1000 Spectrophotometer (Thermo Fisher Scientific, US).



Figure 1: NanoDrop 1000 Spectrophotometer.

The NanoDrop would return an absorbance value of the monomers at a wavelength of 280 nm. This absorbance value can then be used to calculate the total monomer concentration in the supernatant using the Beer-Lambert Law:

$$A = \epsilon C_m l \quad (2.1)$$

In which:

- $A$  = absorbance
- $\epsilon$  = molar extinction coefficient of the protein [ $M^{-1} cm^{-1}$ ]
- $C_m$  = molar monomer concentration [M]
- $l$  = path length (a constant in this case: 1 mm) [cm]

To find the monomer concentration, the equation can be rewritten to the equation 2.2.

$$C_m = \frac{A}{0.1 * \epsilon} \quad (2.2)$$

Since the total protein concentration is a known during the preparation of the proteins, the fibril equivalent monomer concentration can be calculated using equation 2.3.

$$C_f = C - C_m \quad (2.3)$$

In which:

- $C_f$  = molar fibril equivalent monomer concentration [M]
- $C$  = total molar protein concentration [M]
- $C_m$  = molar monomer concentration from supernatant [M]

The NanoDrop spectrophotometer may not be reliable when shown values  $> 1.0$ . To ensure accuracy, absorbance measurements were aimed to be within the range of 0.0 to 0.2, where the instrument operates the most reliably. If undiluted stocks yielded values above this range, they would be diluted appropriately and centrifuged at 18,000 g for 30 minutes, after which the absorbance of the supernatant was measured. The dilution factor should then be accounted for when calculating the concentrations by multiplying the concentrations obtained by the amount the stock was diluted.

Each experiment then focused on evaluating how different amounts of deposited fibrils influenced NP retention. To assess this, the fluorescence emission spectrum of the fluorescent beads passing through each fibril-modified membrane was measured. This allowed for a direct comparison of retention efficiencies at varying fibril deposition levels.

As the goal is to measure the efficiency of each filter with a specific concentration, an emission spectrum of just the solution of the beads would be taken. The beads that have passed the filter, are referred to as the beads filtrate.

### 2.1.5 Physical equipment

To create a filter of protein fibrils, aggregated fibrils were deposited onto polycarbonate Nuclepore track-etched membranes (Avanti Polar Lipids, US) with pore sizes of 0.05  $\mu\text{m}$ , 0.08  $\mu\text{m}$ , 0.4  $\mu\text{m}$ , and 1.0  $\mu\text{m}$ .

To deposit the protein fibril gels onto the membrane, an extruder set (Avanti Polar Lipids, Inc., US) was used, as seen in Figure 2.



Figure 2: Extruder set used to deposit fibrils on the membranes and beads through the fibril-modified filter.

The membrane was first soaked in demineralized water, after which it was placed onto one of the support blocks. Another block was placed on top of it so that the O-Rings on both their surfaces keep it in place. The extruder outer casing and the retained nut were then screwed tightly as to not allow for any movement. A detailed view is shown Figure 3.

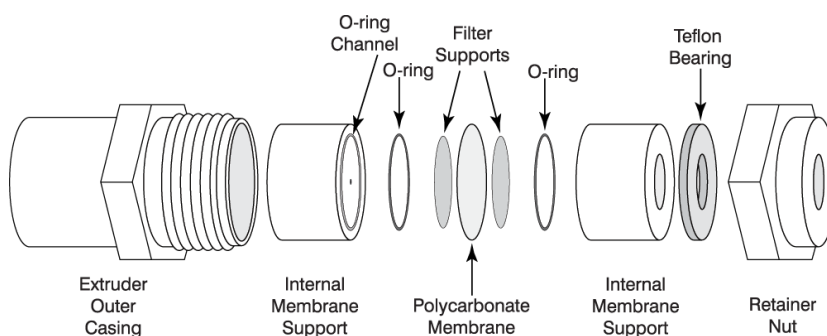


Figure 3: Exploded view of the center part of the extruder set.

An abstract schematic of the deposition process is shown in Figure 4. The fibrils (step 1, green line) were deposited on the polycarbonate membrane (gray ellipse). After this a layer of fibrils is formed on the membrane, shown in step 2. The NPs (step 3, dotted purple line) are then introduced to this fibril layer which should remove them from the suspension, leaving only clean water (step 3, blue line).

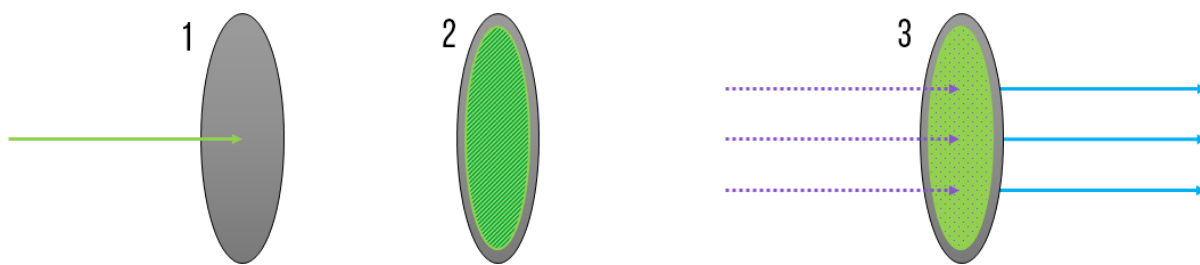


Figure 4: Abstract schematic illustrating the three-step deposition process, including fibril deposition and NP retention.

Two syringes were used for the next process. One was used to deposit the proteins onto the membrane, and the other was used to receive any volume of fibrils that goes through the extruder and passes through the membrane. When the deposition of proteins has finished, the syringes were washed thoroughly with demineralized water and reused to run through the beads for measuring. This was done in a similar manner as the proteins, where one syringe functioned as a deposition syringe and another functioned as the receiving syringe. When the beads solution has been sent through the filter, the then obtained remaining volume in the receiving syringe was then to be saved and measured using a spectrophotometer.

## 2.2 Experimental Data Collection

A spectrophotometer was used to measure the spectra of the beads that passed through the filters. The beads utilized in these experiments were FluoSpheres Carboxylate-Modified Microspheres (Thermo Fisher Scientific, US) with sizes of 0.02  $\mu\text{m}$ , 0.04  $\mu\text{m}$ , and 0.5  $\mu\text{m}$ . These red fluorescent bead suspensions (Ex/Em: 580/605 nm) consist of 1% solids and were further diluted to appropriate concentrations for each experiment. For the 0.04  $\mu\text{m}$  beads, the working concentration was further diluted 40,000x to 8 nM so as to not overflow the spectrophotometer. From here on these beads and any solutions derived from them will be referred to as “beads”.

It is important to note that these beads were from an older stock, raising the possibility of free dye being inside the solution. As free dye could interfere with measurements and retention calculations, each bead suspension was washed prior to use in experiments to minimize the influence of unbound dye on the results. Washing was performed through a multi-step process to remove excess free dye and other impurities from the bead suspension. First, the suspension was centrifuged at 18,000 g for 30 minutes, causing the beads to pellet at the bottom. The supernatant was carefully removed through pipetting without disturbing the pellet and replaced with an equal volume of demineralized water. This process was repeated two additional times.

### 2.2.1 Spectrometer

The emission spectra of the fluorescent beads were obtained using a Varian Cary Eclipse Fluorescence Spectrometer (Agilent Technologies, US). This instrument is equipped with the Cary WinFLR software, which allows precise control over the experimental parameters to achieve spectral data.

For this study, the fluorescence spectrometer was configured with the following key settings:

- Excitation wavelength: 580 nm
- Emission wavelength: 605 nm

- Excitation slit: 5 nm
- Emission slit: 5 nm
- Scan speed: Slow (60 nm/min)
- Photomultiplier voltage: 800 V

These wavelengths were selected to match the excitation and emission peaks of the fluorescent dye in the beads. A slow scan speed was chosen to enhance signal-to-noise ratio.

The Cary WinFLR software facilitated data acquisition and processing. Emission spectra were acquired in .csv format. The retention percentage of the filters would be calculated as follows:

$$Retention\ efficiency = \frac{I_{input} - I_{beads\ filtrate}}{I_{input}} \quad (2.4)$$

In which:

- $I_{input}$  = Intensity of input beads at their emission wavelength of 605 nm. [a.u.]
- $I_{beads\ filtrate}$  = Intensity of beads in filtrate at 605 nm. [a.u.]

## 3 Results and Discussion

### 3.1 Influence of membrane on fluorescent bead retention

In order to measure the efficiency and effectiveness of just the protein fibrils, the membranes should retain as little particles as possible as to not interfere with results. In this set of experiments, the efficiency of membranes was tested by only sending a bead suspension through just a membrane with a set pore size on which no protein fibrils are deposited. The goal here is to find a combination of bead and membrane pore size that influence retention as little as possible. This way the effect of fibrils can be more accurately measured.

#### 3.1.1 Membrane-only retention of 500 nm beads

As seen in Figure 5, membranes themselves also retain fluorescent beads when the pore sizes get within the range of the size of the beads. When these pore sizes get smaller, more beads get retained, up to 96.8% for the smallest pore size membranes. Even when the 500 nm beads should pass through the 1.0  $\mu$ m pore size membrane, 8% still gets retained.

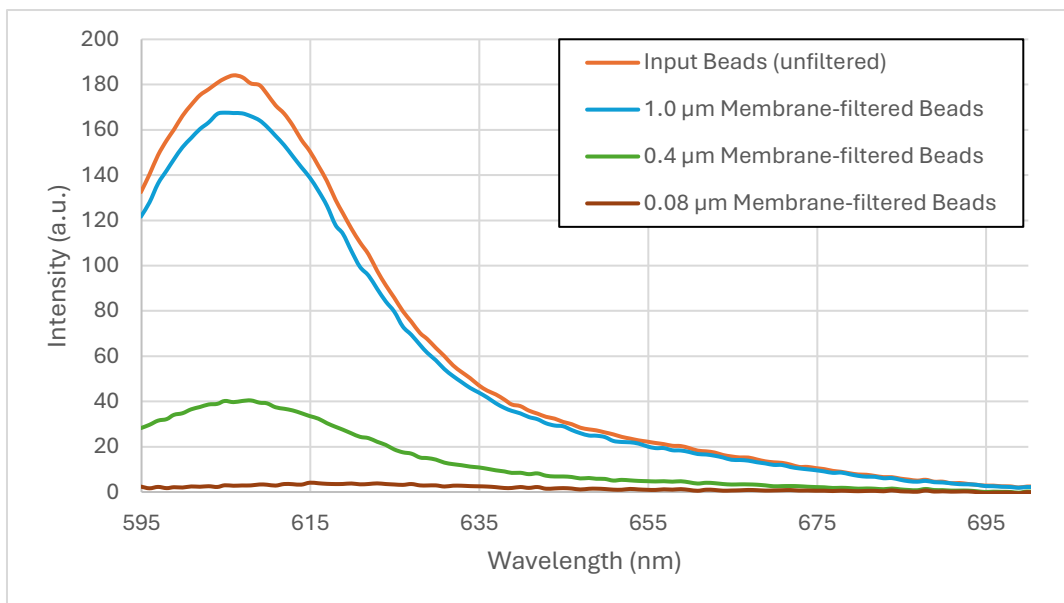


Figure 5: Fluorescence intensity spectrum of a diluted 500 nm fluorescent beads suspension and that same suspension (in orange) after being introduced to membranes with pore sizes of 1.0 µm, 0.4 µm, and 0.08 µm.

Figure 6 shows the exact retention efficiencies of each membrane type. Membranes with pore sizes of 1.0 µm and 0.4 µm retain 8.26% and 78.0% of the beads respectively. The membrane with the smallest pore size of 0.08 µm did not achieve complete retention (100%), but rather only 98.4%, meaning 1.6% still passed through. This 1.6% will be used as a baseline correction and subtracted from future experiments involving retention values. This has also been done for the results in Figure 6.

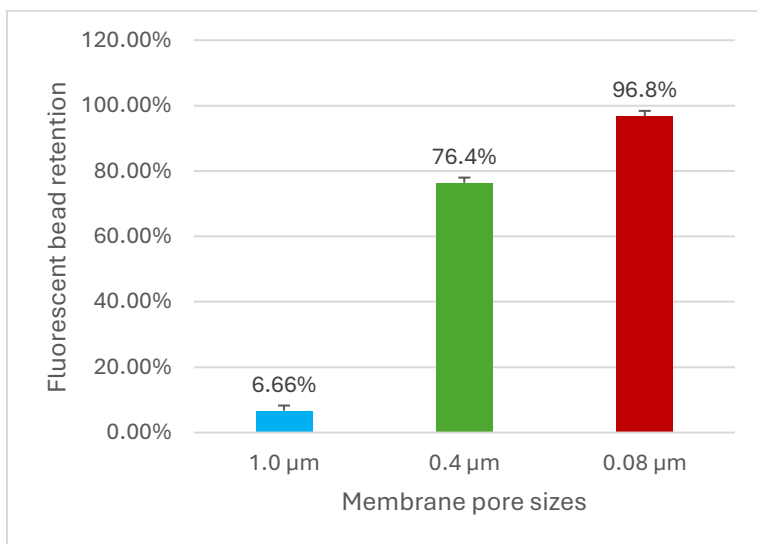


Figure 6: Retention efficiency of 500 nm fluorescent beads using membranes with pore sizes of 1.0 µm, 0.4 µm, and 0.08 µm.

The results depicted in Figure 5 and Figure 6 highlight the relationship between membrane pore size and bead retention efficiency. Note that the baseline correction has been accounted for in this experiment and any future ones. As expected, membranes with smaller pore sizes retain more beads, with the 0.08 µm pore size membrane achieving up to 96.8% retention. This trend aligns

with the principle that pores closer to or smaller than the particle size is more effective at trapping particles due to mechanical sieving.

Interestingly, even the 1.0  $\mu\text{m}$  membrane, which should theoretically allow 500 nm beads to pass through, retains 6.66% of the beads. This suggests the presence of additional factors, like bead aggregation or bead adsorption to the membrane surface, that could contribute to retention.

The 0.4  $\mu\text{m}$  membrane also retained fewer beads than expected (76.4% when baseline correction is applied), despite its pore size being smaller than the 500 nm beads. Ideally, this membrane should have retained nearly all of the beads, but the discrepancy suggests that the actual pore sizes may not strictly be 0.4  $\mu\text{m}$ . Variations in membrane structure, such as irregular pore shapes or non-uniform spacing, may also contribute to this result.

The slight inefficiency of the smallest pore size membrane (96.8%) is likely caused by any free dye molecules in the bead suspension that pass through the pores. These are too small to be retained. Since the beads used had been stored for several years prior to usage in this study, some free dye may have been present in the stock. To remedy this as much as possible, the diluted beads solution was washed with demineralized water as much as possible. The baseline correction of 1.6% that is caused by this remaining free dye that could not be washed down will be considered for future experiments.

### 3.1.2 Membrane-only retention of 40 nm beads

When using 40 nm beads and introducing them into membranes with varying pore sizes, none of them retain beads. Figure 7 shows the intensity spectrum of the 40 nm beads after they have passed through each of the membrane types. There is no meaningful difference between each of the membranes, showing that using 40 nm will result in the membrane having as little influence on the retention of beads as possible. However, the fluorescence spectrum of the 1.0  $\mu\text{m}$  pore size membrane closely matches that of the unfiltered beads, indicating minimal retention.

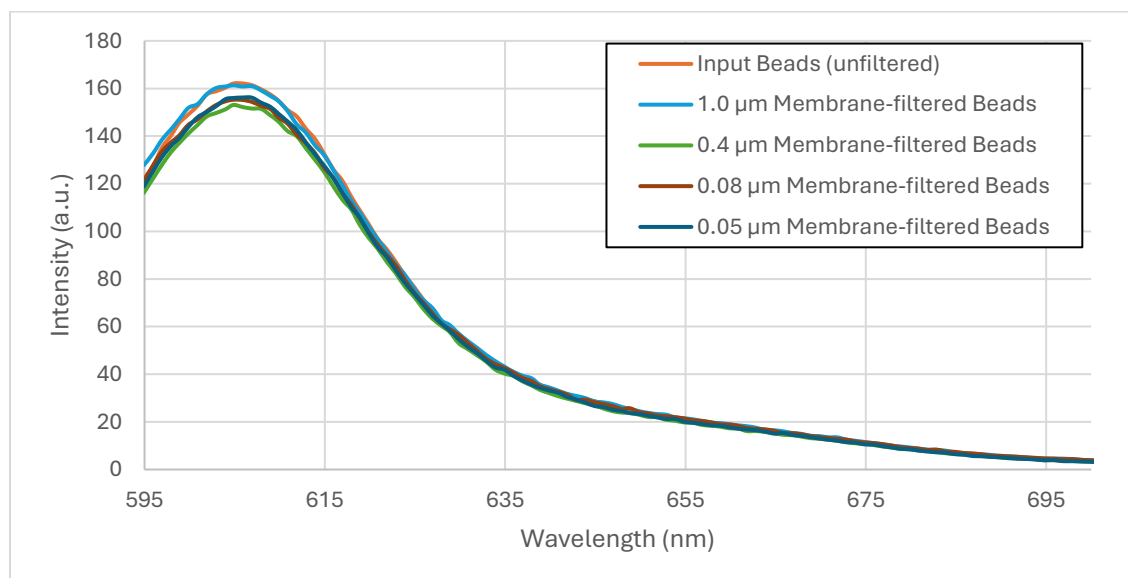


Figure 7: Fluorescence intensity spectrum of 0.04 nM 40 nm fluorescent bead suspension and that same suspension (in orange) after being introduced to membranes with pore sizes of 1.0  $\mu\text{m}$ , 0.4  $\mu\text{m}$ , 0.08  $\mu\text{m}$ , and 0.05  $\mu\text{m}$ .

Figure 8 further shows that 1.0  $\mu\text{m}$  pore size membranes retain the least beads, with the other three options showing some more retention, while still being more efficient than 500 nm beads sent through a membrane with 1.0  $\mu\text{m}$  pore size.

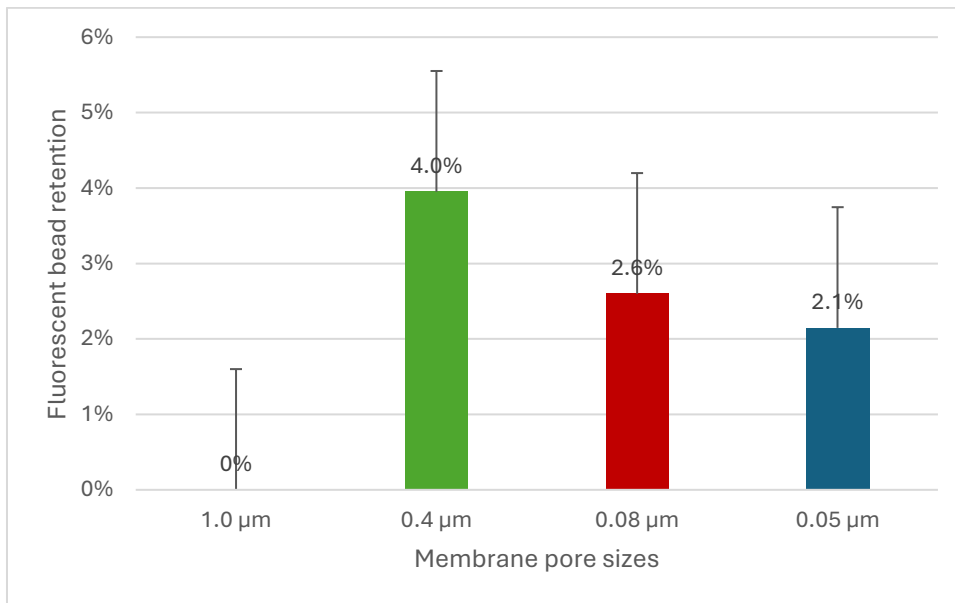


Figure 8: Retention efficiency of 40 nm fluorescent beads using membranes with pore sizes of 1.0  $\mu\text{m}$ , 0.4  $\mu\text{m}$ , 0.08  $\mu\text{m}$ , and 0.05  $\mu\text{m}$ .

When accounted for the baseline correction, the 1.0  $\mu\text{m}$  pore size membrane only showed a retention rate of 0%. Interestingly, the amount of beads retained decreases as the pore sizes get smaller, while the opposite would be expected.

The results shown in Figure 7 and 12 show that membrane pore size has little influence on the retention of 40 nm beads. Across all membrane types, the retention efficiencies are minimal, with the 1.0  $\mu\text{m}$  pore size membrane showing optimal retention. The fluorescence spectrum of the beads after passing through the 1.0  $\mu\text{m}$  pore size membrane, shown in Figure 7, closely matches the spectrum of the input, indicated in orange. This suggests that the 1.0  $\mu\text{m}$  introduces minimal interference, and this can be confirmed by looking at the retention efficiency of that membrane in Figure 12.

This low retention confirms that the 40 nm beads can freely pass through the membranes, regardless of pore size, as none are sufficiently small to trap these beads effectively. Notably, the amount of retention seen in Figure 8 shows that the retention decreases as pore sizes get smaller when theoretically the opposite should happen. However, since this is shown to happen within the baseline correction of 1.6%, it can be attributed to experimental variability rather than a trend, suggesting that differences in retention in this instance are not meaningful and likely result from minor inconsistencies.

While the 0.4  $\mu\text{m}$ , 0.08  $\mu\text{m}$ , and 0.05  $\mu\text{m}$  should not have significant impact on the retention efficiency of experiments, to ensure accuracy, the 1.0  $\mu\text{m}$  pore size membrane was chosen in combination with 40 nm 8 nM fluorescent beads to be used in further experiments.

### 3.2 Monitoring protein fibrillation using Thioflavin T assay

To determine whether fibrils have formed, and if a protein can create fibrils, a Thioflavin T (ThT) assay was performed. When binding to fibrils ThT fluoresces strongly, thus giving a relatively accurate early indication of fibril formation. In this assay, low counts indicate poor fibril formation and high counts indicate strong fibril formation.

Do note that ThT becomes self-fluorescent at concentrations of approximately 5  $\mu\text{M}$  and higher, according to Khurana et al. [17]. This suggests that only BSA would contain a ThT concentration that borders on this limit, while the other preparations might be at risk of interference from ThT self-fluorescence. Since the starting concentrations of each protein differs a 1:20 ratio was used to still allow for comparison between the proteins, shown in Table 3. However, Figure 9 demonstrates that even at 500  $\mu\text{M}$  ThT in tris buffer – a concentration 100 times higher than the supposed self-fluorescence threshold – no significant fluorescence signal was observed. This suggest that, under the conditions in this study, ThT does not contribute to fluorescence intensity on its own, contrary to what was reported by Khurana et al. [17]. Whatever the exact cause, this is an encouraging result, as it confirms that fluorescence signals observed in this study primarily originate from fibril-bound ThT rather than free ThT fluorescence.

Initially, five proteins were considered to make fibrils, each at specific conditions. To verify if these proteins can form fibrils, we resorted to the use of the ThT fluorescence assay. This method is effective because ThT fluoresces strongly upon binding to fibrils, providing an early indication of fibril formation.

Figure 9 shows initial ThT assay results indicating fibril formation. All proteins aside from lysozyme (pH 7.5) showed sufficient fibril formation or saw an increase in fibrils after one day. It is important to note that while lysozyme (pH 7.5) did not show significant fibril formation. This is because it was too early for  $\alpha$ -synuclein to form fibrils at this point and was omitted from Figure 9 because of this. Fibril formation of  $\alpha$ -synuclein would be validated at a later time and confirmed.

Since lysozyme (pH 7.5) showed a decrease in fibrils and low fluorescence after one day, it would not be used for further experiments. While Insulin and  $\beta$ -lactoglobulin (pH 7.5) also showed a decrease in fibrils after one day, its fluorescence counts remained sufficient to warrant further experimentation. High counts suggest the presence of at least some degree of amyloid-like structures. These two protein types would be monitored closely to observe any anomalous behavior regarding fibrillation.

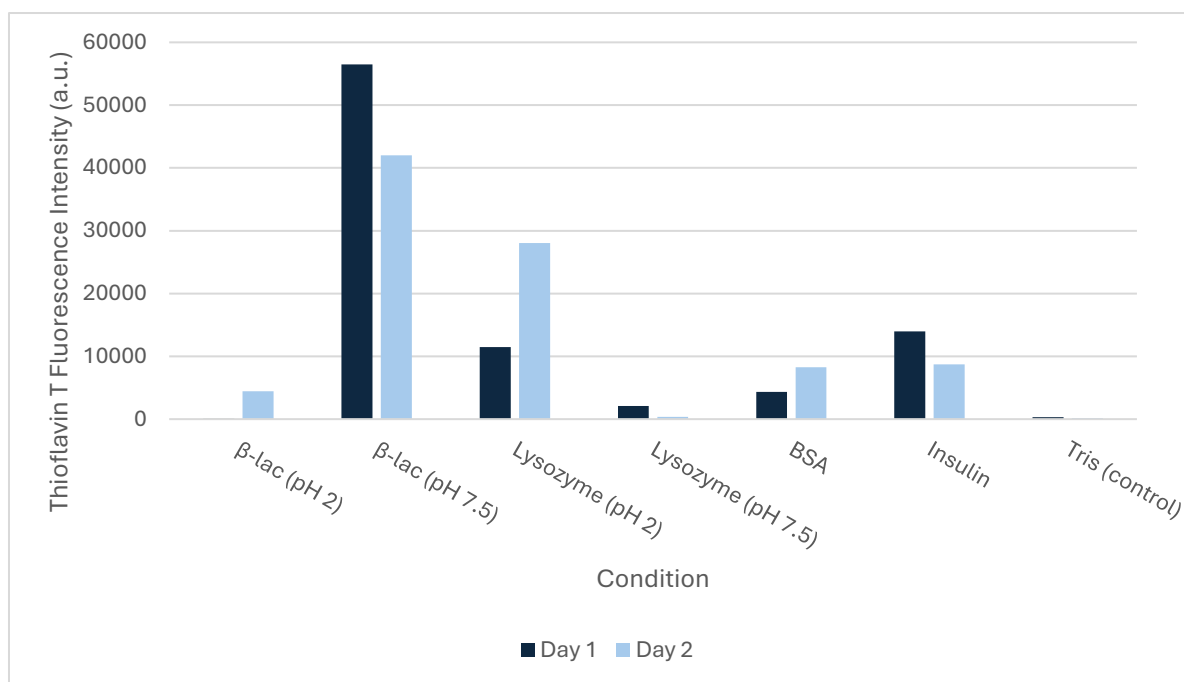


Figure 9: Early ThT assays indicating fibril formation via Thioflavin T fluorescence at various time intervals.

The initial ThT assay results showed fibril formation for all tested proteins, bar lysozyme (pH 7.5), insulin, and  $\beta$ -lactoglobulin (pH 7.5), which showed a decrease in fibrils over time. The decrease in fibril formation for lysozyme at pH 7.5 shows the critical role of pH in amyloid fibril formation. It directly influences protein charge and the interactions that drive fibrillation. At pH 7.5, lysozyme may be closer to its isoelectric point, where net charge is minimal. This in turn could potentially favor irregular aggregation over organized fibrillation. This aligns with previous findings showing that acidic conditions (i.e., pH 2) improve lysozyme fibrillation by increasing the protein's net positive charge, promoting intermolecular attractions and fibril formation [14, 15].

However, the reduction in fibril content over time at pH 7.5 cannot be solely attributed to pH itself. It could be influenced by secondary processes such as fibril disassembly or degradation. A study by Stepanenko et al. (2021) shows that factors such as enzymatic activity and environmental conditions can influence lysozyme fibrils formed at a neutral pH to undergo degradation over time [18]. The decrease in fibrillation seen in insulin and  $\beta$ -lactoglobulin (pH 7.5) may similarly be attributed to suboptimal pH-conditions and time-dependent degradation processes.

### 3.2.1 Characterizing Fibril Morphology with AFM

To confirm the presence of fibrils and assess their structural characteristics, Atomic Force Microscopy (AFM) images were captured for both remaining fibril types at a concentration of 70 nmol, as shown in Figure 10. While these images confirm fibril formation, it is important to note that the substrate used for AFM imaging (mica) differs from the polycarbonate membranes used in deposition experiments. Consequently, the results are indicative of fibril characteristics but may not directly represent fibril deposition on membranes.

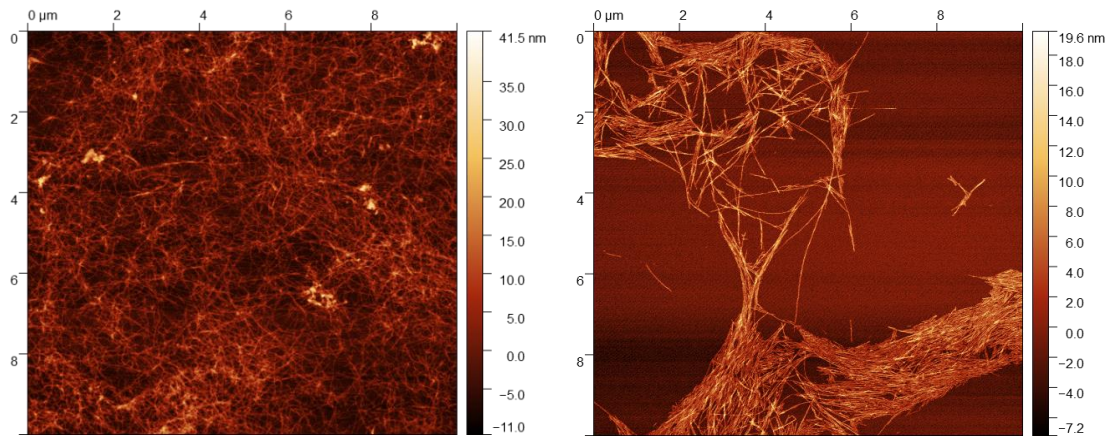


Figure 10: AFM images of 70 nmol fibrils deposited on a surface: lysozyme (left) and  $\alpha$ -synuclein (right). The images reveal distinct surface height variations caused by the presence of fibrils, highlighting differences in their structural morphology and coverage. Note the difference in the y-axis scale: the lysozyme fibril deposition exhibits heights more than double those of the  $\alpha$ -synuclein fibrils.

The lysozyme fibrils (left image in Figure 10) appear more evenly distributed across the membrane surface, forming a relatively uniform layer. In contrast, the  $\alpha$ -synuclein fibrils (right image in Figure 10) display a less uniform deposition, with large areas of empty space combined with regions of dense fibril clusters interspersed with large empty areas. The differences in structural morphology are further reflected in the height profiles, visible on the y-axis of Figure 10.

### 3.2.2 Preliminary Analysis of Protein Filter Performance

To assess whether fibril-modified membranes can retain fluorescent nanobeads, an experiment was conducted in which fluorescent beads were sent through fibril-modified membranes. First, fibrils were deposited onto the membranes at an equal concentration for all tested proteins to ensure comparability. After fibril deposition, a 0.5 mL solution of fluorescent beads was passed through each membrane. The filtrate was then collected and transferred into separate cuvettes for measurement using a spectrophotometer. The input bead solution was also measured.

The primary assumption in this experiment is that fluorescence intensity is directly correlated with the concentration of fluorescent nanobeads. This assumption is maintained throughout the thesis, as the study focuses on a model system where fluorescence intensity serves as an indirect measure of nanoplastic retention efficiency. A reduction in fluorescence after filtration indicates successful retention by the fibril layer. By taking the fluorescence intensity values of the filtered beads at their emission wavelength of 605 nm and comparing that to the same intensity values of the input beads, retention values could be evaluated.

The results of these experiments are shown in Figure 11 and Figure 13. From these intensity values, a retention value can be calculated. Fluorescent beads were measured both before filtration (in orange) and after passing through a fibril-modified membrane. Concentrations for each tested protein were equal to allow for comparison between them.

Based on the observed fluorescence intensity spectra, the tested proteins were categorized in two groups: those performing measurable retention of beads and those displaying inconsistent results. This separation allows for a more focused analysis of the proteins which do retain beads, while proteins exhibiting inconsistent results were set aside for further investigation or excluded for further use.

Of the six protein types that remain, only lysozyme at pH 2 (hereafter referred to only as lysozyme),  $\beta$ -lactoglobulin at pH 2, and  $\alpha$ -synuclein show meaningful fluorescent bead retention, shown in Figure 11 and Figure 12. The fluorescence intensity of the beads after they have passed through each of the protein filters is lower than the beads themselves, shown in Figure 11.

The “Beads” curve is consistently higher than the other three, indicating a reduction in fluorescence intensity as a result of filtration. Among the three fibril-modified membranes, the curves for  $\beta$ -lactoglobulin (pH 2), and  $\alpha$ -synuclein are closely clustered, with lysozyme being slightly lower than the other two. All three of these protein types seem effective at filtering and retaining fluorescent beads.

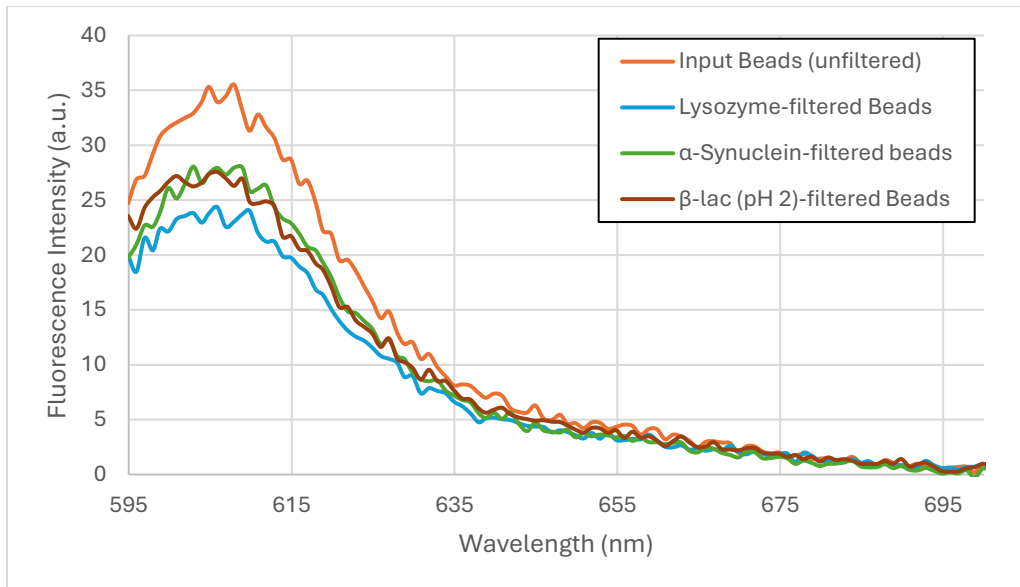


Figure 11: Fluorescence intensity spectrum of diluted solution of 20 nm beads, and that same bead suspension (in orange) after passing through lysozyme,  $\beta$ -lactoglobulin (pH 2), and  $\alpha$ -synuclein fibril-modified 1.0  $\mu\text{m}$  pore size membrane.

Of the three protein types, lysozyme-modified membranes exhibit the highest retention efficiency (31.0%), outperforming both  $\beta$ -lactoglobulin (pH 2) and  $\alpha$ -synuclein significantly, shown in Figure 12. This suggests that lysozyme fibrils have stronger interactions with the beads or a stronger fibril network for retention.

When accounting for the baseline correction, both  $\beta$ -lactoglobulin (pH 2) and  $\alpha$ -synuclein have similar retention efficiencies (20.9% and 20.7% respectively), potentially indicating that their fibril structure or surfaces interact in a similar manner with the fluorescent beads.

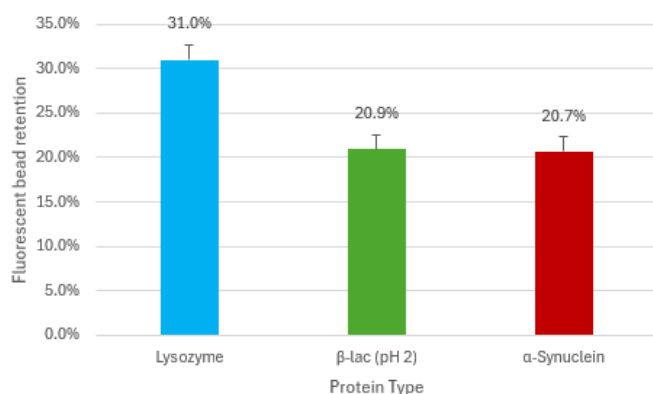


Figure 12: Retention efficiency of 20 nm fluorescent beads using lysozyme,  $\beta$ -lactoglobulin (pH 2), and  $\alpha$ -synuclein fibril-modified 1.0  $\mu\text{m}$  pore size membranes.

Lysozyme at pH 2 performed the highest with regards to retention efficiency (31.0%), which can be attributed to several factors. Firstly, at pH 2, lysozyme forms highly stable fibrils. These networks are more uniform and interconnected, making it more difficult for nanoparticles to pass through the filtration layer with fewer gaps. AFM imaging in similar studies has shown that lysozyme fibrils form smoother and more consistent layers compared to other proteins [15]. This can also be seen in Figure 10, which shows an AFM image of lysozyme. Another reason is that lysozyme fibrils carry a significant positive charge at acidic pH, enhancing electrostatic interactions with negatively charged nanoparticles. This aligns with studies that show that the surface charge of both the fibrils and particles being filtered is often linked to the retention efficiency of fibrils [14].

The retention efficiencies for  $\beta$ -lactoglobulin (20.9%) and  $\alpha$ -synuclein (20.7%) were similar, suggesting possible parallels in their binding mechanisms and structural properties. However, differences in their fibril formation and network characteristics may explain their comparable but distinct retention behaviors.

Fibrils derived from  $\beta$ -lactoglobulin at pH 2 tend to form long, unbranched, often twisted structures [30]. This reduced network density creates gaps that allow NPs to pass through, lowering retention efficiency. Comparatively,  $\alpha$ -synuclein are known for their variability in structure, and often form dense clusters in areas while covering other areas scarcely. This uneven distribution may stem from surface-catalyzed secondary nucleation, where the surface of existing fibrils nucleates the formation of new, independent fibrils, resulting in inconsistent coverage [19]. It can form highly stable fibrils, but also exhibits a high variability in fibril morphology, possibly hindering its ability to form consistent layers [14].

Figure 13 illustrates the intensity spectrum of the second anomalous group, consisting of  $\beta$ -lactoglobulin (pH 7.5), Insulin, and BSA. The spectrum of beads filtered through  $\beta$ -lactoglobulin (pH 7.5) fibrils is notably irregular, lacking the classic peak structure at 600 nm typically seen in fluorescent bead spectra, suggesting the presence of an additional fluorescent species or increased scattering. This scattering may be caused by larger particles or aggregates in the filtrate, which could have resulted from membrane fracture or improper filtration. In contrast, the spectrum of beads filtered through BSA fibrils more closely resembles the expected pattern but exhibits noticeable scattering in the 595–605 nm range, indicative of larger particles or aggregates.

The beads passing through the insulin fibril exhibit a typical spectrum, but the intensity is not lower than that of the beads prior to filtration, suggesting the insulin retains few, if any, beads.

The irregular results observed for  $\beta$ -lactoglobulin (pH 7.5) may be linked to the absence of  $\text{NaN}_3$  during preparation.  $\text{NaN}_3$  acts as a preservative to prevent bacterial growth, and its omission could have resulted in microbial contamination. This in turn could have led to particle aggregation or the presence of unexpected fluorescent species in the filtrate.

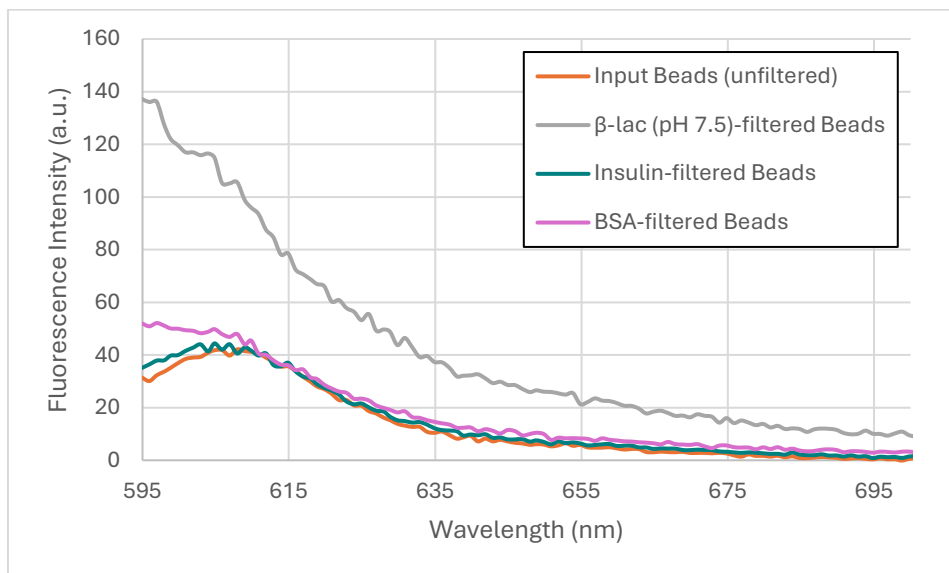


Figure 13: Fluorescence intensity spectrum of diluted solution of 20 nm beads, and that same bead suspension (in orange) after passing through a  $\beta$ -lactoglobulin (pH 7.5), insulin, and BSA fibril-modified 1.0  $\mu\text{m}$  pore size membrane.

The fluorescence spectra in Figure 13 indicate that none of the tested protein-modified membranes effectively retained fluorescent beads. Instead, the signal intensity in the filtrate for certain samples, particularly  $\beta$ -lactoglobulin (pH 7.5), appears unusually high compared to the input beads. This suggests the presence of additional fluorescent species or interference effects. Previous studies have reported similar influences due to scattering, aggregation, or unexpected fluorescence contributions from the protein aggregates themselves [8]. The elevated intensity in the  $\beta$ -lactoglobulin sample suggests that it is not a viable candidate for effective bead retention. Likewise, the spectra for BSA and insulin do not indicate significant retention, as their fluorescence profiles closely follow that of the beads in the input. Since their intensity is largely the same as the input beads, with what may be scattering around 595-605 nm in the BSA, they are similarly not fit to be used for bead retention.

Given the inconsistent nature of the initial results,  $\beta$ -lactoglobulin (pH 7.5), Insulin, and BSA were excluded from further experiments involving fluorescent bead filtration. Future experiments should ensure proper membrane integrity and the inclusion of  $\text{NaN}_3$  to prevent similar issues.

### 3.3 Evaluating Fibril Performance in Filtration

#### 3.3.1 Retention Efficiency with Increasing Fibril Concentration

Figure 14 presents the results of an experiment in which the concentration of deposited fibrils was increased across five measurements: 1.07 nmol, 2.14 nmol, 4.28 nmol, 8.55 nmol, and 17.1 nmol of deposited fibrils. When depositing the fibrils on the membrane, 1 mL of solution was deposited

each time. For this experiment, the assumption is made that all fibrils in the solution are successfully deposited onto the membrane surface during the 1 mL deposition step. This assumption equates the concentration of deposited fibrils to the original concentration of the solution multiplied by the volume deposited. This calculation does not account for potential losses.

Bead retention was recorded at each concentration point, with the goal of identifying trends in retention efficiency as the amount of fibrils on the membrane surface increased.

Initially,  $\alpha$ -synuclein and lysozyme both exhibit retention below zero, with  $\beta$ -lactoglobulin first reaching a negative retention at 4.28 nmol deposited fibrils. This theoretically should be impossible, as it would imply that additional particles are created beyond those initially passed through. Ideally, the retention efficiency should have increased with fibril concentration for all protein types, with all retention values remaining positive.

However, the results deviated significantly from these expectations. Initially,  $\alpha$ -synuclein and lysozyme both exhibit negative values, with  $\alpha$ -synuclein never reaching positive retention values. The  $\beta$ -lactoglobulin filter initially displayed a slight decrease in retention, followed by a sharp drop to approximately -80% at the third measurement. After this point, retention gradually improved but did not surpass 0%.

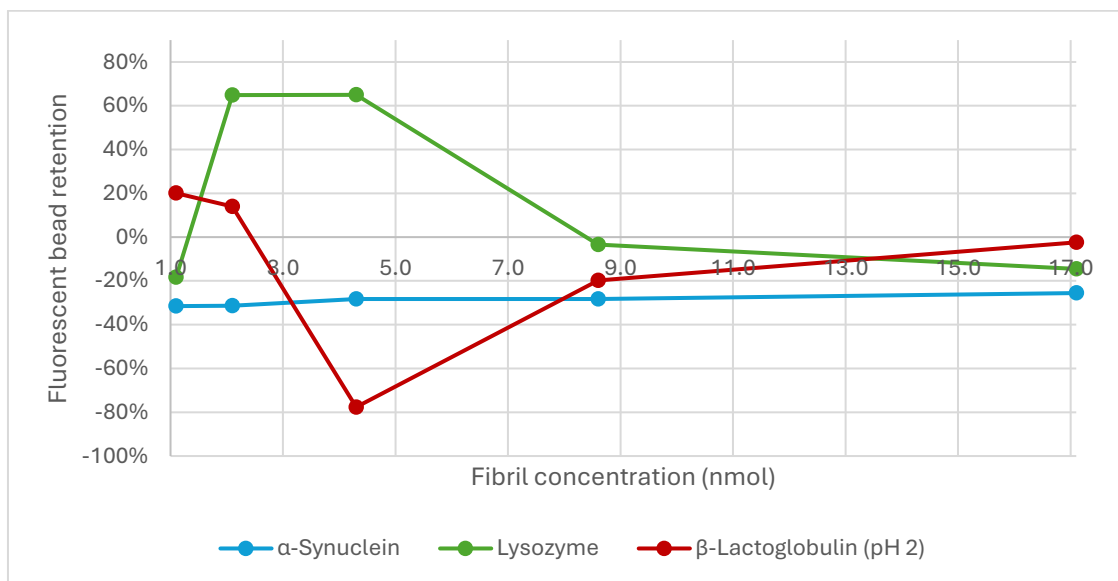


Figure 14: Retention efficiency of 20 nm fluorescent beads at varying fibril concentrations (1.07 – 17.1 nmol) for  $\alpha$ -synuclein, lysozyme, and  $\beta$ -lactoglobulin (pH 2). Data shows differences in retention trends among the protein fibrils.

A factor to consider is the possibility of structural issues arising during the deposition process. If the membrane developed microfractures or other inconsistencies during this process, it could have let through larger aggregates or beads past the fibril layer. This could also lead to irregular flow patterns that prevent the proper retention. The unexpected behavior shown in Figure 14 might also be attributed to differences in the actual amount of deposited fibrils on the membrane compared to the theoretical calculations. Variability in the deposition process could result in less fibrils on the membrane than intended, theoretically resulting in less retention efficiency.

As these results are inconsistent and do not align with expected behavior, further investigation was conducted into potential factors of influence, including the membrane itself and whether the actual amount of fibrils deposited on the membrane matches the theoretical calculated value.

### 3.3.2 Quantifying fibril deposition

To determine the fraction of fibrils and monomers passing through the membrane during deposition, an experiment as performed using absorbance measurements of the filtrate before and after treatment with guanidinium chloride (GuHCl). The goal of this experiment was to quantify how much fibril content remains in the filtrate, and therefore is not deposited on the membrane, and to compare it to the theoretical expectation that fibrils, being larger than the membrane pores, should not pass through.

This approach relied on the known concentrations of fibril preparations (735  $\mu\text{M}$  for lysozyme and 333  $\mu\text{M}$  for  $\beta$ -lactoglobulin) and utilized GuHCl to denature and unfold the fibrils back into monomers, herein enabling accurate total protein quantification in the filtrate. The experiment involved two key measurements:

1. Filtrate treated with GuHCl, which provides the total protein concentration in the filtrate.
2. Filtrate post-centrifugation (without GuHCl), which allows quantification of monomer concentration only.

The fraction of fibrils retained on the membrane is calculated as the difference between the total protein concentration (GuHCl-treated filtrate) and the monomer concentration (centrifuged filtrate), multiplied by the 1 mL volume of deposited solution. GuHCl was used at a concentration of 6 M, and absorbance was measured at 280 nm.

Figure 15 shows the absorbance of lysozyme (73.5 nmol fibrils) and  $\beta$ -lactoglobulin (66.6 nmol fibrils) before and after filtration. After filtration, a slight increase in absorbance was observed for both proteins following GuHCl treatment when compared to the filtrate samples that underwent centrifugation, indicating a presence of fibrils in the filtrate. This suggests that fibrils passed through the membrane, likely due to structural issues.

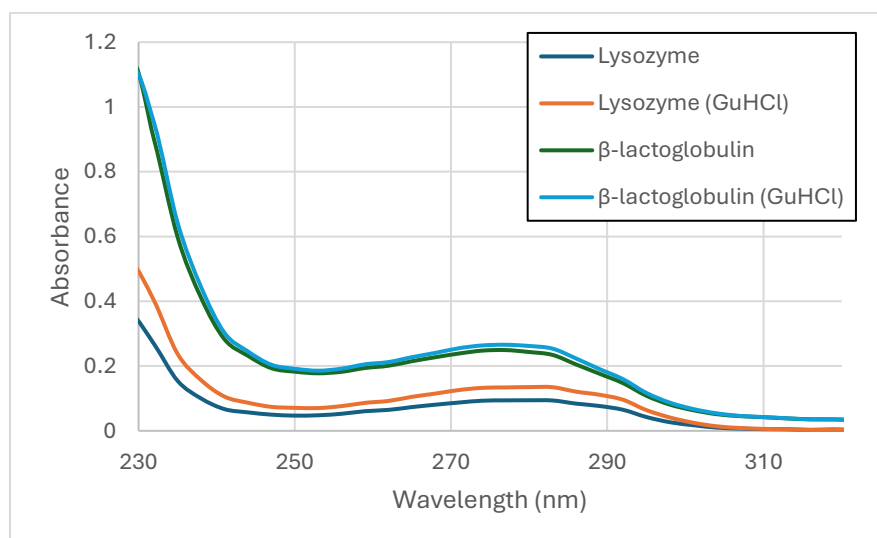


*Figure 15: Absorbance measurement of lysozyme and  $\beta$ -lactoglobulin that have been deposited on the membrane and taken up after the fact. The figure shows this filtrate before and after it has been treated with GuHCl and after it has been centrifuged.*

While GuHCl has a minor impact on absorbance at this wavelength ( $\leq 0.02$ , according to Thermo Fischer Scientific [20]), the addition of 6 M GuHCl increases the total sample volume, which might still influence the absorbance readings. This increase in volume may therefore influence the absorbance readings, as the signal reflects not only the protein content, but also the added GuHCl solution. Consequently, more experiments should be performed to determine the deposition process and membrane stability.

### 3.3.3 Visualizing Fibril Deposition and Membrane Stability

This experiment examines the deposition of labeled  $\alpha$ -synuclein and ThT onto a 1.0  $\mu\text{m}$  pore size membrane, with the aim of assessing the deposition process and identifying any inconsistencies that could affect experimental results. The goal of this experiment was to understand how fibrils interact with the membrane during deposition and whether factors, such as the experimental setup or membrane structure, influence the effectiveness of fibril deposition.

When imaging the membrane on which  $\alpha$ -synuclein labeled with Alexa Fluor 568 has been deposited, it can be seen that there is no uniform deposition. Figure 16 highlights a significant accumulation of labeled proteins at the edges of the membrane, which is where the membrane is clamped by the support rings. This suggests that the design of the setup might influence the distribution of fibrils during the deposition process. The proteins appear to be drawn toward these areas, possibly due to mechanical constraints or uneven flow during application. This accumulation at the edges could create regions of higher fibril density, leading to non-uniform filtration performance and potentially affecting the membrane's retention efficiency.

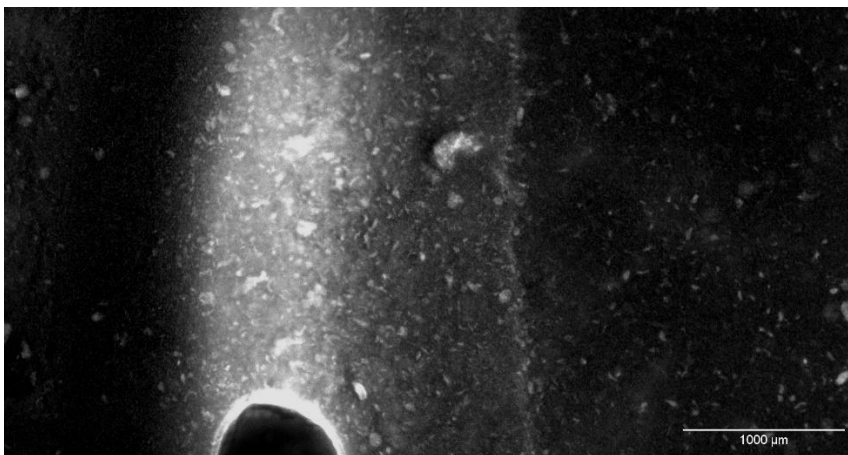


*Figure 16: Left edge of a 1.0  $\mu\text{m}$  pore size membrane on which  $\alpha$ -synuclein labeled with Alexa Fluor 568 has been deposited. Accumulation of proteins on the edges can be observed.*

The middle of the membrane, as imaged in Figure 17 shows a clear divide in terms of fibril density, indicated by the red line. The distribution of fibrils also is sparser than on the edges of the membrane. This irregular deposition could result from the method used to apply the fibrils, as the membrane is positioned vertically during the process rather than horizontally. Additionally, when the membrane is removed from the support blocks, any loose proteins that have not adhered to

the membrane may shift downward due to gravity, further contributing to the non-uniform deposition.

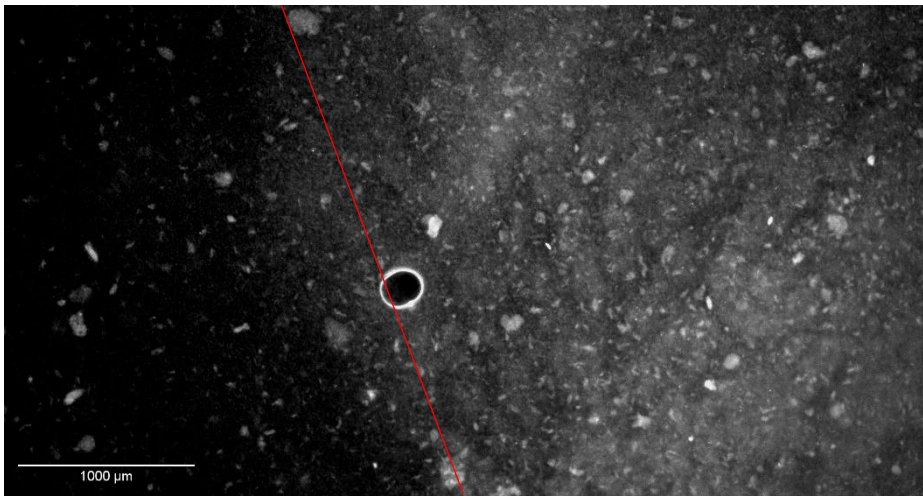


*Figure 17: Center of a 1.0 μm pore size membrane on which α-synuclein labeled with Alexa Fluor 568 has been deposited. A clear divide can be observed in the middle of the membrane, possibly indicating that deposition of the protein is not uniform.*

Another identical 1.0 μm membrane was imaged after ThT was deposited on it, with the result shown in Figure 18. The image, taken from the center of the membrane, reveals that the membrane had torn. This tearing likely resulted from challenges encountered during the deposition process.

Depositing fibrils onto the membrane created significant pressure, making it initially difficult to empty the syringe. Applying high pressure was needed to overcome this resistance, but it also meant that the membrane was under considerable stress. When sufficient pressure was applied, it would suddenly release, allowing the syringe to be emptied with ease. This sudden change in pressure was an early indication that there were underlying issues with the membrane's integrity. Such difficulties were compounded by the lack of a support layer between the membrane and the supporting blocks, leaving the membrane vulnerable to tearing.

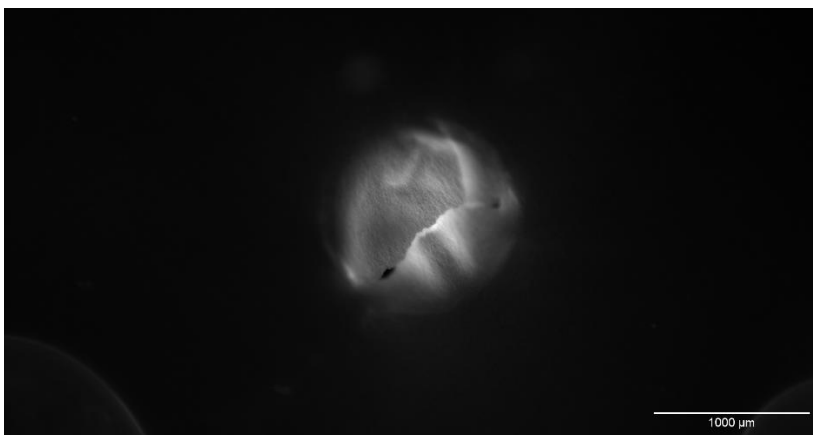


*Figure 18: Center of a 1.0 μm pore size membrane on which ThT has been deposited. A break within the membrane can be observed.*

The imaging results in Figure 18 present a clear issue with membrane integrity during deposition of fibrils and beads. The tear observed in the 1.0 μm indicates that pressure buildup within the

supporting blocks surpassed the membrane's mechanical tolerance. The difficulty in emptying the syringe when initially depositing fibrils further supports this, as the sudden ease of fluid flow likely corresponds to the moment the membrane ruptures. This is shown with an abstract schematic in Figure 19.

Since the middle blocks contain only a single channel for fluid flow, the pressure causes the membrane to rupture, allowing the fluid to pass through. As the input fluid (arrow) is sent through the blocks and interacts with the membrane (gray line), a pressure is created and the membrane is pushed down onto the supporting block, shown in image 2 of Figure 19. This pressure keeps building up until the membrane breaks in the middle. This then allows the input fluid to easily flow into the singular channel in the supporting block. Without a support layer beneath the membrane, there is little structural reinforcement, increasing the likelihood of tearing.

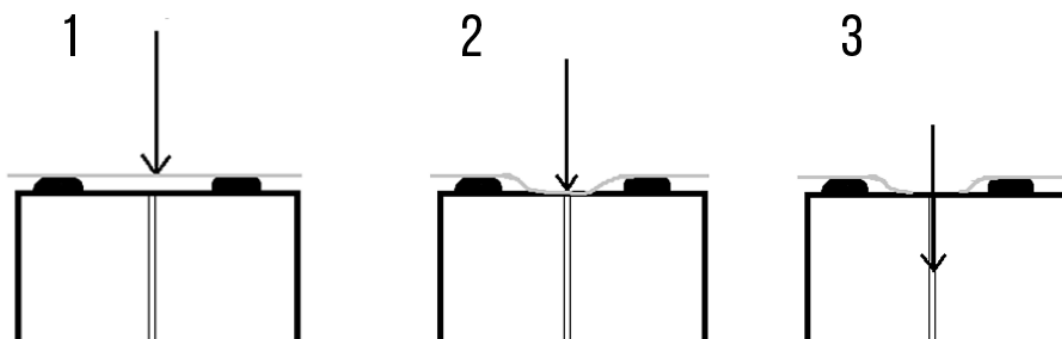


Figure 19: Illustration of the deposition process leading to membrane rupture.

To address this issue, a filter support layer was introduced to the receiving end of the extruder setup, as illustrated in Figure 3. This support layer is designed to fit precisely within the rings, filling the space between the membrane and the surface of the supporting block, as shown in image 1 of Figure 19. This slows down the fluid deposition process but ensures that the membrane remains intact by preventing excessive pressure buildup. The addition of the support layer would ensure more consistent fibril deposition and improve the reliability of the experimental results.

### 3.4 Determining protein retention performance trends

To evaluate the retention performance of  $\alpha$ -synuclein and lysozyme fibril-modified membranes, an experiment was conducted in which fluorescent bead concentration was varied while keeping the amount of deposited fibrils constant at 70 nmol. This allowed for assessment of how fibrils interact with increasing nanoplastic loads and whether retention efficiency trends could be observed. A fixed volume of 0.5 mL of input bead solution was used in each measurement to ensure consistency across conditions.

The membrane structure issue was resolved by adding a support layer, ensuring the membrane remains intact during the experiment.

The selected proteins were  $\alpha$ -synuclein and lysozyme at pH 2. The  $\beta$ -lactoglobulin sample was excluded from further testing due to the presence of larger aggregates that were not solely fibrils. This left just  $\alpha$ -synuclein and lysozyme for testing. Other proteins were excluded during experimentation due to anomalies, inconsistencies, or other factors warranting their elimination.

The fibril concentration in the  $\alpha$ -synuclein aggregated sample was determined to be 220  $\mu\text{M}$ , while the lysozyme aggregated sample contained 287  $\mu\text{M}$  of fibrils. These were diluted to the same concentration for deposition to more accurately draw comparisons between the two proteins.

Note that retention efficiencies (percentages) are measured here, as opposed to the amount of particles. This is due to the central assumption of this thesis that the fluorescent intensity of the beads is directly proportional to the amount of beads.

### 3.4.1 $\alpha$ -Synuclein fibril-modified membrane

Fluorescent bead retention by  $\alpha$ -synuclein fibrils increased by up to 48 percentage points with a fluorescent bead concentration of 0.32 nM as shown in Figure 20. The overall curve increases sharply when concentrations are low, but the increase in retention efficiency slows down as bead concentrations rise, reaching up to 94% retention.

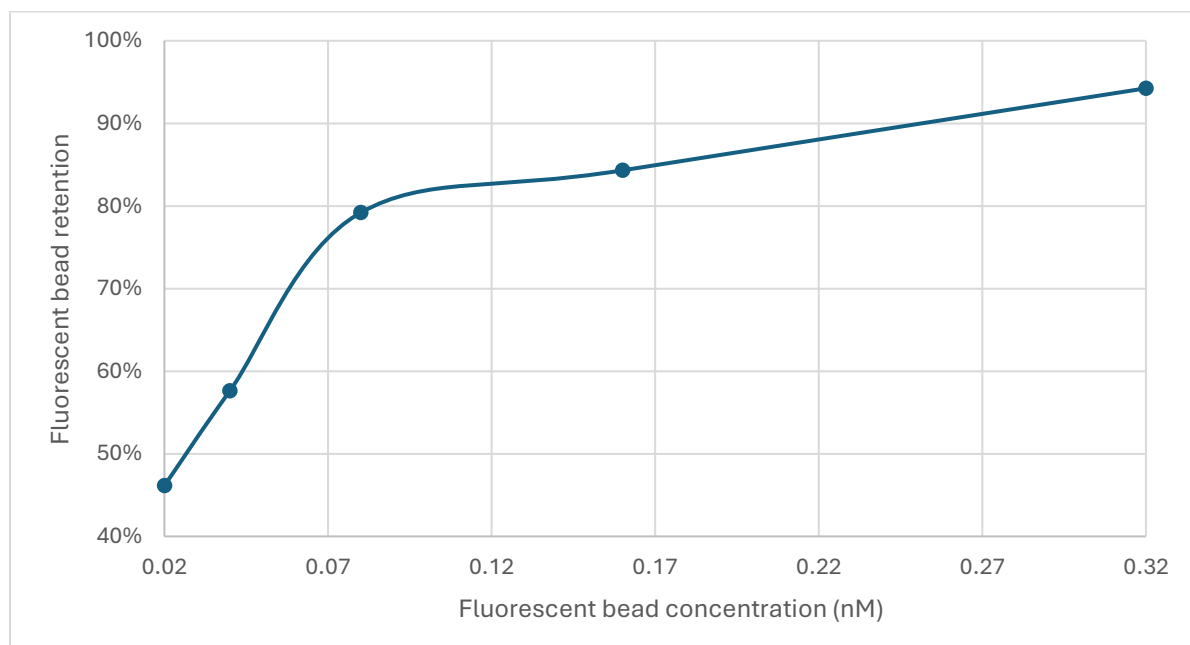


Figure 20: Retention of 40 nm fluorescent beads by a 70 nmol  $\alpha$ -synuclein fibril-modified membrane across bead concentrations in the 0.02 – 0.32 nM range.

Hydrophobic interactions play a critical role in strengthening  $\alpha$ -synuclein fibril networks. At physiological and acidic pH, the exposed hydrophobic domains of  $\alpha$ -synuclein interact strongly. In the case of this thesis,  $\alpha$ -synuclein was prepared at a physiological pH (7.5) using Tris. Though  $\alpha$ -synuclein contains both hydrophobic and hydrophilic domains, a stiffer and more cohesive network is formed mainly due to the hydrophobic domains interacting dominantly [21, 22], enhancing its ability to trap nanoplastics through hydrophobic forces [14].

### 3.4.2 Lysozyme fibril-modified membrane

Though still retaining beads, the lysozyme fibril-modified membrane consistently demonstrated lower retention, reaching a maximum of 22% at the highest bead concentration (0.32 nM), as shown in Figure 21. Retention sharply increased at lower bead concentrations but flattened significantly as concentrations rose, resembling a binding curve. Notably, at a bead concentration of 0.16 nM, retention decreased before continuing this trend.

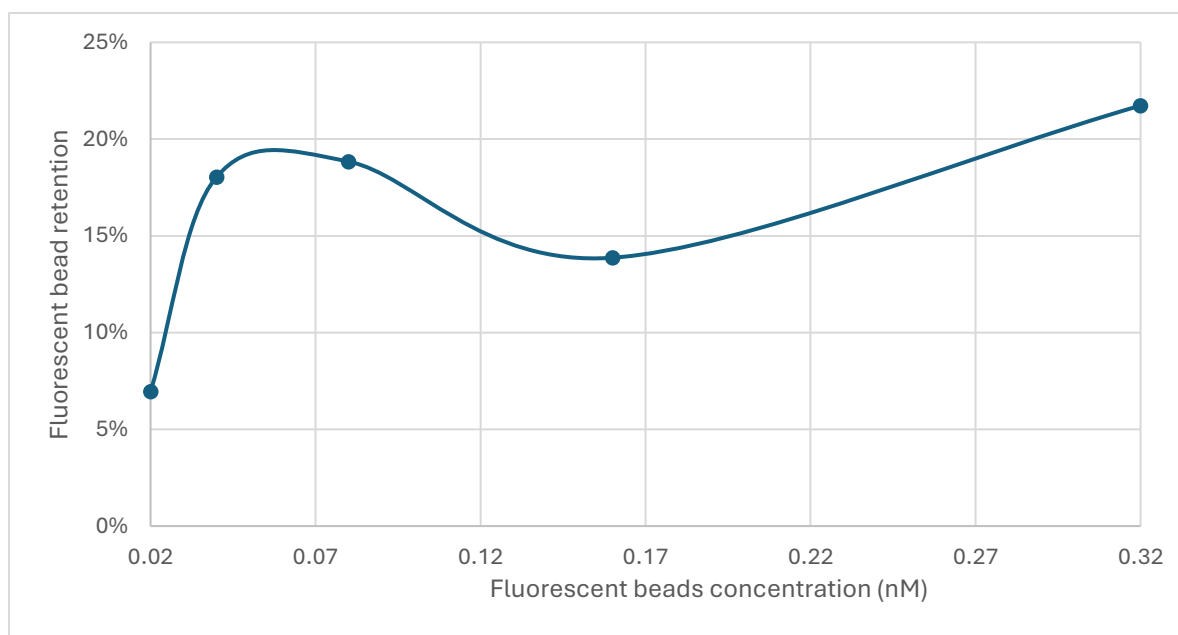


Figure 21: Retention of 40 nm fluorescent beads by a 70 nmol lysozyme fibril-modified membrane across bead concentrations in the 0.02 - 0.32 nM range.

The results in Figure 20 and Figure 21 highlight the differences between  $\alpha$ -synuclein and lysozyme fibril-modified membranes. The significantly higher retention achieved by  $\alpha$ -synuclein fibrils (up to 94%) compared to lysozyme fibrils (22%) can be attributed to their ability to self-assemble into dense and cohesive networks. As shown by Semerdzhiev et al. (2014) [21],  $\alpha$ -synuclein fibrils form supra-fibrillar networks with increased stiffness and interconnectivity.

Lysozyme fibrils, while effective to a degree, lack the same structural density and interconnectivity as  $\alpha$ -synuclein. A study by Mikalauskaite et al. (2022) [23] showcases that lysozyme fibrils formed at higher temperatures (65°C in this study) exhibit reduced beta-sheet-rich fibrillar structures, instead potentially transitioning into different aggregate types with increased structural ability and non-amyloid structures [23]. This structural variability may hinder their ability to form robust filtration layers. Additionally, the binding of lysozyme with nanoplastics relies primarily on only hydrophobic interactions [14], which are less versatile than the combined hydrophobic and electrostatic mechanisms seen in  $\alpha$ -synuclein fibrils [21].

However, another study performed by Taylor et al. (2021) [31] shows complete opposite trends that the ones shown in these results, with particle transmission strongly increasing as the particle throughput increases. The results shown in Figure 20 and Figure 21 would indicate that particle transmission decreases with increasing particle throughput. Taylor et al. (2021) suggested that as binding sites become saturated with particles, the percentage of particles retained may decrease as unbound particles pass through the filter more freely [31]. It would suggest that more particles are passing through the filter, and fewer are being captured or retained. This decrease in efficiency may be due to factors such as clogging or pore blocking as a result of the increasing concentration of particles.

The discrepancy between the results shown and those of Taylor et al. (2021) [31] could have multiple reasons. Firstly, a study by Cho et al., (2024) [32] show that smaller particles exhibit significantly higher uptake and transport compared to larger particles. Particles used in Taylor et

al. (2021)'s study were within the size range of 100-400 nm, whereas the particles used in the present study were 40 nm large.

Moreover, considering after support was added, the deposition process took longer. This means that flow rate also decreased as a result of adding the support layer. Tränkle et al. (2016) investigated the interaction dynamics of diffusing particles and how contact times may be influenced by flow rates [33]. The lower flow rate in the present study may therefore cause longer contact times between the fluorescent nanoparticles and the fibrils.

Another study by Blum et al. (2016) [34] shows that dense, interconnected networks may resist clogging and maintain pore structure integrity under high particle loads. The fibrils used in this experiment may exhibit similar properties. Multiple studies have researched  $\alpha$ -synuclein's ability to form these cohesive networks [14, 21, 22]. This would also explain the discrepancy between lysozyme and  $\alpha$ -synuclein, as  $\alpha$ -synuclein would have a denser and more interconnected fibril network when compared to lysozyme [23].

## 4 Conclusion

This study has demonstrated the potential of amyloid-like protein fibrils as effective materials for nanoplastic retention. Among the tested fibril-modified membranes,  $\alpha$ -synuclein outperformed lysozyme, achieving up to 94% bead retention compared to 22% retention with lysozyme fibrils. The superior performance of  $\alpha$ -synuclein fibrils can be attributed to their ability to form denser and more interconnected networks, as supported by AFM imaging and previous studies on fibril assembly. Comparatively, lysozyme's retention efficiency was limited by its structural variability.

However, the discrepancies observed between the current results and those of Taylor et al. (2021) may be attributed to differences in particle sizes, flow rates, and structural properties of the fibrils. Smaller nanoparticles, slower flow rates, and stronger fibril interactions may contribute to the increase retention efficiency observed in this study.

Future research should not only focus into quantifying fibril-bead interactions, but also investigate the underlying mechanisms behind the unexpected high retention in this study more precisely. This includes analyzing how variations in fibril network density, structural integrity, and interaction strength contribute to retention efficiency.

Additionally, examining the role of different flow rates and particle sizes in influencing retention outcomes will provide valuable insights. Understanding these factors will aid in refining fibril design and enhancing the practical applications of fibril-modified membranes in mitigating nanoplastic pollution in environments.

## References

- [1] Geyer, R., Jambeck, J. R., & Law, K. L. (2017). *Production, use, and fate of all plastics ever made*. <https://doi.org/10.1126/sciadv.1700782>
- [2] Zaman, A., & Newman, P. (2021). Plastics: are they part of the zero-waste agenda or the toxic-waste agenda? *Sustainable Earth*, 4(1). <https://doi.org/10.1186/s42055-021-00043-8>
- [3] Rani-Borges, B., & Ando, R. A. (2024). How small a nanoplastic can be? A discussion on the size of this ubiquitous pollutant. *Cambridge Prisms: Plastics*, 2, e23. <https://doi.org/10.1017/plc.2024.25>
- [4] Zurub, R. E., Cariaco, Y., Wade, M. G., & Bainbridge, S. A. (2023). Microplastics exposure: implications for human fertility, pregnancy and child health. In *Frontiers in Endocrinology* (Vol. 14). Frontiers Media SA. <https://doi.org/10.3389/fendo.2023.1330396>
- [5] Kopatz, V., Wen, K., Kovács, T., Keimowitz, A. S., Pichler, V., Widder, J., Vethaak, A. D., Hollóczy, O., & Kenner, L. (2023). Micro- and Nanoplastics Breach the Blood–Brain Barrier (BBB): Biomolecular Corona’s Role Revealed. *Nanomaterials*, 13(8). <https://doi.org/10.3390/nano13081404>
- [6] Manke, A., Wang, L., & Rojanasakul, Y. (2013). Mechanisms of nanoparticle-induced oxidative stress and toxicity. In *BioMed Research International* (Vol. 2013). <https://doi.org/10.1155/2013/942916>
- [7] Ojha, P. C., Satpathy, S. S., Ojha, R., Dash, J., & Pradhan, D. (2024). Insight into the removal of nanoplastics and microplastics by physical, chemical, and biological techniques. *Environmental Monitoring and Assessment*, 196(11), 1055. <https://doi.org/10.1007/s10661-024-13247-0>
- [8] Jachimowicz, P., & Cydzik-Kwiatkowska, A. (2022). Coagulation and Flocculation before Primary Clarification as Efficient Solutions for Low-Density Microplastic Removal from Wastewater. *International Journal of Environmental Research and Public Health*, 19(20). <https://doi.org/10.3390/ijerph192013013>
- [9] Ahmed, M. B., Rahman, M. S., Alom, J., Hasan, M. S., Johir, M. A. H., Mondal, M. I. H., Lee, D. Y., Park, J., Zhou, J. L., & Yoon, M. H. (2021). Microplastic particles in the aquatic environment: A systematic review. *Science of The Total Environment*, 775, 145793. <https://doi.org/10.1016/J.SCITOTENV.2021.145793>
- [10] Talvitie, J., Mikola, A., Koistinen, A., & Setälä, O. (2017). Solutions to microplastic pollution – Removal of microplastics from wastewater effluent with advanced wastewater treatment technologies. *Water Research*, 123, 401–407. <https://doi.org/10.1016/J.WATRES.2017.07.005>
- [11] Hidayaturrehman, H., & Lee, T. G. (2019). A study on characteristics of microplastic in wastewater of South Korea: Identification, quantification, and fate of microplastics during treatment process. *Marine Pollution Bulletin*, 146, 696–702. <https://doi.org/10.1016/J.MARPOLBUL.2019.06.071>

- [12] Toyama, B. H., & Weissman, J. S. (2011). Amyloid structure: Conformational diversity and consequences. *Annual Review of Biochemistry*, 80, 557–585. <https://doi.org/10.1146/annurev-biochem-090908-120656>
- [13] Knowles, T. P. J., & Mezzenga, R. (2016). Amyloid fibrils as building blocks for natural and artificial functional materials. In *Advanced Materials* (Vol. 28, Issue 31, pp. 6546–6561). Wiley-VCH Verlag. <https://doi.org/10.1002/adma.201505961>
- [14] López, E. F., Gabbrielli, S., Colnaghi, L., Mazzuoli-Weber, G., Cesare, A., Redaelli, L., & Gautieri, A. (2023). *Academic Editors: Carolina Nebot molecules In Silico Analysis of Nanoplastics' and  $\beta$ -amyloid Fibrils' Interactions*. <https://doi.org/10.3390/molecules28010388>
- [15] Peydayesh, M., & Mezzenga, R. (n.d.). *Protein nanofibrils for next generation sustainable water purification*. <https://doi.org/10.1038/s41467-021-23388-2>
- [16] Jin, T., Peydayesh, M., Joerss, H., Zhou, J., Bolisetty, S., & Mezzenga, R. (2021). Environmental Science Water Research & Technology Amyloid fibril-based membranes for PFAS removal from water †. *Cite This: Environ. Sci.: Water Res. Technol*, 7, 1873. <https://doi.org/10.1039/d1ew00373a>
- [17] Khurana, R., Coleman, C., Ionescu-Zanetti, C., Carter, S. A., Krishna, V., Grover, R. K., Roy, R., & Singh, S. (2005). Mechanism of thioflavin T binding to amyloid fibrils. *Journal of Structural Biology*, 151(3), 229–238. <https://doi.org/10.1016/J.JSB.2005.06.006>
- [18] Stepanenko, O. v., Sulatsky, M. I., Mikhailova, E. v., Stepanenko, O. v., Kuznetsova, I. M., Turoverov, K. K., & Sulatskaya, A. I. (2021). Trypsin induced degradation of amyloid fibrils. *International Journal of Molecular Sciences*, 22(9). <https://doi.org/10.3390/ijms22094828>
- [19] Thacker, D. I., Barghouth, M. I., Bless, M., Zhang, E., & Linse, S. (2023). *Direct observation of secondary nucleation along the fibril surface of the amyloid 42 peptide*. <https://doi.org/10.1073/pnas>
- [20] 8M Guanidine-HCl solution. Thermo Fisher Scientific - US. (n.d.). <https://www.thermofisher.com/order/catalog/product/24115>
- [21] Semerdzhiev, S. A., Dekker, D. R., Subramaniam, V., & Claessens, M. M. A. E. (2014). Self-assembly of protein fibrils into suprafibrillar aggregates: Bridging the nano- and mesoscale. *ACS Nano*, 8(6), 5543–5551. <https://doi.org/10.1021/nn406309c>
- [22] Semerdzhiev, S. A., Lindhoud, S., Stefanovic, A., Subramaniam, V., van der Schoot, P., & Claessens, M. M. A. E. (2018). Hydrophobic-Interaction-Induced Stiffening of  $\alpha$ -Synuclein Fibril Networks. *Physical Review Letters*, 120(20). <https://doi.org/10.1103/PhysRevLett.120.208102>
- [23] Mikalauskaite, K., Ziaunys, M., & Smirnovas, V. (2022). *Lysozyme Amyloid Fibril Structural Variability Dependence on Initial Protein Folding State*. <https://doi.org/10.3390/ijms23105421>
- [24] Tang, Y., Zhang, S., Su, Y., Wu, D., Zhao, Y., & Xie, B. (2021). Removal of microplastics from aqueous solutions by magnetic carbon nanotubes. *Chemical Engineering Journal*, 406, 126804. <https://doi.org/10.1016/J.CEJ.2020.126804>

- [25] Enfrin, M., Lee, J., Gibert, Y., Basheer, F., Kong, L., & Dumée, L. F. (2020). Release of hazardous nanoplastic contaminants due to microplastics fragmentation under shear stress forces. *Journal of Hazardous Materials*, 384, 121393. <https://doi.org/10.1016/J.JHAZMAT.2019.121393>
- [26] Zhang, Y., Diehl, A., Lewandowski, A., Gopalakrishnan, K., & Baker, T. (2020). Removal efficiency of micro- and nanoplastics (180 nm–125 µm) during drinking water treatment. *Science of The Total Environment*, 720, 137383. <https://doi.org/10.1016/J.SCITOTENV.2020.137383>
- [27] Wang, Z., Lin, T., & Chen, W. (2020). Occurrence and removal of microplastics in an advanced drinking water treatment plant (ADWTP). *Science of The Total Environment*, 700, 134520. <https://doi.org/10.1016/J.SCITOTENV.2019.134520>
- [28] Gao, W., Zhang, Y., Mo, A., Jiang, J., Liang, Y., Cao, X., & He, D. (2022). Removal of microplastics in water: Technology progress and green strategies. *Green Analytical Chemistry*, 3. <https://doi.org/10.1016/j.greeac.2022.100042>
- [29] Peydayesh, M., Suta, T., Usuelli, M., Handschin, S., Canelli, G., Bagnani, M., & Mezzenga, R. (2021). Sustainable Removal of Microplastics and Natural Organic Matter from Water by Coagulation-Flocculation with Protein Amyloid Fibrils. *Environmental Science and Technology*, 55(13), 8848–8858. <https://doi.org/10.1021/acs.est.1c01918>
- [30] Loveday, S. M., Rao, M. A., Creamer, L. K., & Singh, H. (n.d.). *Factors Affecting Rheological Characteristics of Fibril Gels: The Case of  $\beta$ -Lactoglobulin and  $\alpha$ -Lactalbumin*. <https://doi.org/10.1111/j.1750-3841.2009.01098.x>
- [31] Taylor, N., Ma, W., Kristopeit, A., Wang, S. C., & Zydney, A. L. (2021). Evaluation of a sterile filtration process for viral vaccines using a model nanoparticle suspension. *Biotechnology and Bioengineering*, 118(1), 106–115. <https://doi.org/10.1002/BIT.27554>
- [32] Cho, Y., Seo, E. U., Hwang, K. S., Kim, H., Choi, J., & Kim, H. N. (2024). Evaluation of size-dependent uptake, transport and cytotoxicity of polystyrene microplastic in a blood-brain barrier (BBB) model. *Nano Convergence*, 11(1), 40. <https://doi.org/10.1186/s40580-024-00448-z>
- [33] Tränkle, B., Ruh, D., & Rohrbach, A. (2016). Interaction dynamics of two diffusing particles: Contact times and influence of nearby surfaces. *Soft Matter*, 12(10), 2729–2736. <https://doi.org/10.1039/c5sm03085d>
- [34] Blum, K. M., Novak, T., Watkins, L., Neu, C. P., Wallace, J. M., Bart, Z. R., & Voytik-Harbin, S. L. (2016). Acellular and cellular high-density, collagen-fibril constructs with suprafibrillar organization. *Biomaterials Science*, 4(4), 711–723. <https://doi.org/10.1039/c5bm00443h>